processes

MDPI

Article

Structural Design and Simulation Analysis of a Dual-Row Pneumatic Vegetable Precision Planter

Yanjun Li [1], Yang Bai [1], Xunlin Zhang [2] and Fuxiang Xie [1,*]

[1] School of Machinery and Automation, Weifang University, Weifang 261000, China; liyanjun@wfu.edu.cn (Y.L.); baiyang19891014@163.com (Y.B.)
[2] School of Mechanical and Electronic Engineering, Shandong University of Science and Technology, Qingdao 266590, China; xunlin1995@163.com
* Correspondence: xfx608@126.com; Tel.: +86-177-0636-5915

Abstract: In order to solve the problems of domestic and foreign vegetable precision metering devices that easily damage seeds and have low seeding efficiency and poor qualification rate, this paper designs a one-machine for two-row pneumatic combination seeder, which is mainly composed of a pneumatic seeding mechanism and a honeycomb seeding mechanism. The mechanism and other components and theoretical analysis of the working process of the combined seed metering device clarifies the minimum negative pressure for adsorbing a seed during the suction stage, along with the negative pressure required for the seed-carrying stage. It also establishes the seeding speed and movement during planting with the trajectory parameter equation and uses ADAMS software to conduct virtual experiments on the influence of the number of holes, diameters, and heights of different types of honeycomb seeding disks on the success rate of seeding. Based on research on previous pneumatic seeding mechanisms, single factor tests, orthogonal tests, and high-speed photography tests of the honeycomb seeding disk of the combined seeder were carried out on the number of holes, the diameter of holes, and the height of seeding. The results of tests conducted on okra seeds showed that when the rotating speed of the pneumatic seeding disc was 18 r/min, the diameter of the pneumatic seeding disc hole was 2.4 mm, the vacuum degree was 3.5 kPa, the number of honeycomb seeding disc holes was 24, the hole diameter was 13 mm, and the seed height was 60 mm, the working performance of the combined seed meter reached the optimal level, which provides a reference for the development of a small seed vegetable precision seeder.

Keywords: small seeds; precision seeder; combined seed meter; virtual simulation; experiment

Citation: Li, Y.; Bai, Y.; Zhang, X.; Xie, F. Structural Design and Simulation Analysis of a Dual-Row Pneumatic Vegetable Precision Planter. *Processes* **2023**, *11*, 1803. https://doi.org/10.3390/pr11061803

Academic Editor: Ireneusz Zbicinski

Received: 18 May 2023
Revised: 8 June 2023
Accepted: 12 June 2023
Published: 14 June 2023

1. Introduction

With different operating principles, seeding apparatus can be mechanical or pneumatic [1]. The former feeds and drops the seeds based on the mechanical structure, which can be inclined, vertical, or horizontal disc types; socket wheel type; or finger clamp type [2,3]. However, mechanical structures may damage the seeds, lower their germination rate, and reduce the qualification rate of seeding, so that mechanical apparatus is not applicable for precision seeding. Pneumatic seeders can be divided into vacuum type, blowing type, pressure type, or roller type. They all rely on the structure of the seed plate and the action of the airflow to complete the process of seed collection and dropping [4,5]. However, the number and diameter of seed holes are prone to seeding failure, significantly affecting the seeding performance. It is worth noting that both pneumatic and mechanical seeding apparatuses have a low qualification rate of seeding.

Research on vegetable sowing technology and equipment began earlier in foreign countries than in China, and the level of automation and intelligence is higher [6]. For example, Maschio developed a multifunctional pneumatic vegetable sowing machine to improve the versatility of the sowing unit and enable the sowing of seeds with different

diameters. In Japan and South Korea, small and medium-sized mechanical seeders with power support are mainly used, and their overall structure is compact and lightweight. They are mostly suitable for sowing seed pellets, such as the YAZAKI SYV-M600W vegetable sowing machine, but the small holes of the nest wheel sower are prone to clogging with dust and impurities [7]. Seeders in foreign countries are expensive and the cost of sowing is high, and they have not been widely promoted and applied in China. China's research in vegetable sowing technology and equipment started relatively late. Based on the introduction and digestion of advanced foreign technology, various types of small and medium-sized vegetable sowing equipment have been developed, but the theory and technology of sowing are not mature enough, and the performance and efficiency of sowing equipment both still need to be improved [8]. The DB series vegetable sowing machine produced by Deere Play Agricultural Machinery Company has good versatility but has problems with high seed breakage rate and has serious sowing leakage. Tian et al. [9] developed a rapeseed joint sowing machine to improve sowing efficiency, using a combination of positive and negative pressure sowing, with a qualified sowing rate of 90%. Wang et al. [10] developed a circumferential groove seam air suction precision sowing machine for seeding grains, with a replanting index of less than 15% and a sowing leakage index of less than 8%.

The above analysis reveals that seeding apparatus is the core component of a vegetable precision planter. Many foreign and domestic studies have analyzed precision seeding apparatuses by focusing on pneumatic or mechanical seeding alone in single-row precision seeding. However, combined seeding apparatus that can seed in two rows has rarely been looked at. Considering the advantages and disadvantages of mechanical and pneumatic seeders at home and abroad, this paper designs a pneumatic combination precision seeder for small vegetable seeds based on the analysis of the sowing mechanism. It can simultaneously sow two rows, thereby reducing operating costs and improving sowing efficiency. Therefore, precision seeders that can sow multiple rows at the same time have broad market prospects.

2. The Structure and Operating Principle of the Combined Seeding Apparatus

The combination seeder is mainly composed of a pneumatic seed separation mechanism and a honeycomb seed separation mechanism, while the most commonly used precision vegetable seeders mainly use pneumatic or mechanical seed separation mechanisms. The pneumatic seed separation mechanism designed in this paper mainly uses the pressure difference to adsorb the seeds on a pneumatic seed plate, while the honeycomb seed separation mechanism mainly uses the gravity of the seeds to complete the sowing operation. The combined use of the two mechanisms can achieve one-machine for two-row precision sowing, as shown in Figure 1.

2.1. Design of Critical Components

2.1.1. Pneumatic Seeding Mechanism

The pneumatic seeding mechanism consists of a left-end cover, a right-end cover, a seed storage box, a seed scraping plate, a seed stirring wheel, a fixed frame for the seed stirring wheel, a seed blocking plate, a seed dropping plate, a pneumatic seeding plate, a sealing ring, a sealing plate, and a fixing piece for the sealing plate (Figure 2).

(1) Pneumatic seeding disc

The structure of the pneumatic seeding disc is illustrated in Figure 3. As demonstrated, its major parameters include the diameter of the seeding disc and the shape, diameter, number, and position of the holes. The diameter of the seeding disc is closely related to the overall size of the seeding apparatus, the linear speed of the seeding disc, and the centripetal force required by the seed. Therefore, an equation set was established to analyze the influence of the seeding disc on seed performance.

$$\begin{cases} t = \frac{l_c}{v} \\ l_c = \theta \frac{D}{2} \\ 60s = 2\pi n \frac{D}{2} \end{cases} \quad (1)$$

where: t—time of pneumatic seeding disc turning through the seeding area, s; l_c—arc length of the seeding area, mm; v—linear speed of the pneumatic seeding disc, m/s; D—diameter of the seeding disc, mm; θ—radius of the seeding area, rad; n—rotational speed of the pneumatic seeding disc, r/min.

$$t = \frac{30\theta}{\pi n} \quad (2)$$

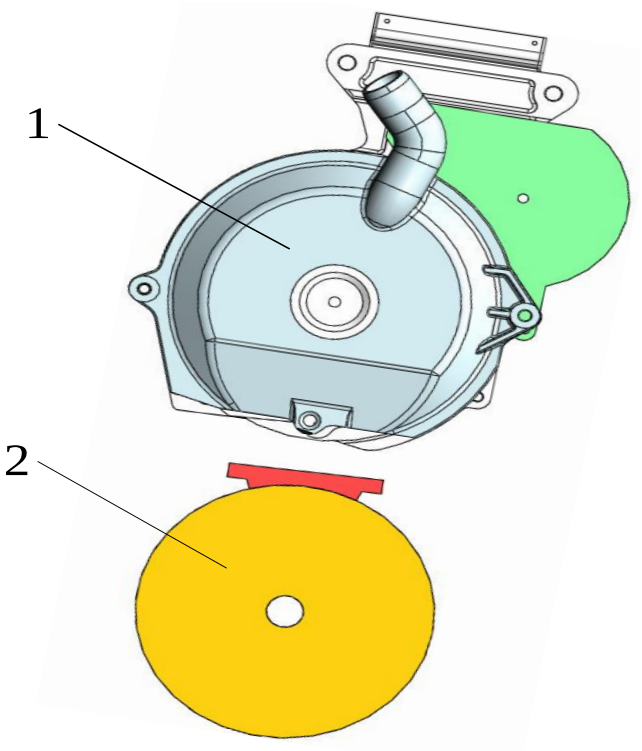

Figure 1. Combined seed metering device. 1. Pneumatic seeding mechanism; 2. Honeycomb seeding mechanism.

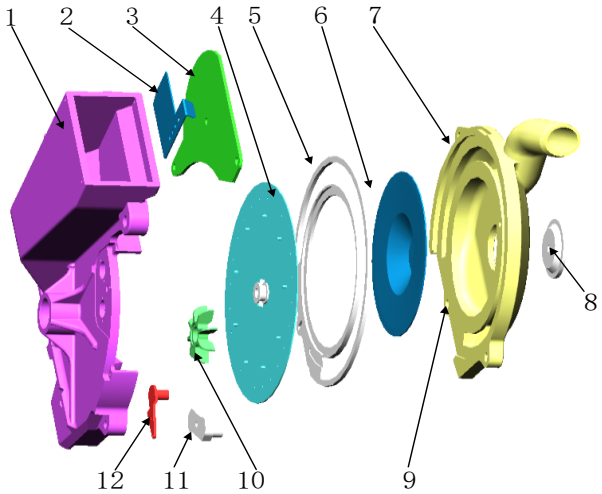

Figure 2. Pneumatic seeding mechanism. 1. seed storage box; 2. seed stopper; 3. seed scraper; 4. seed row disc; 5. seal ring; 6. seal disc; 7. negative pressure inlet; 8. gasket; 9. positive pressure hole; 10. seed stirring wheel; 11. seed paddle; 12. seed stirring wheel bracket.

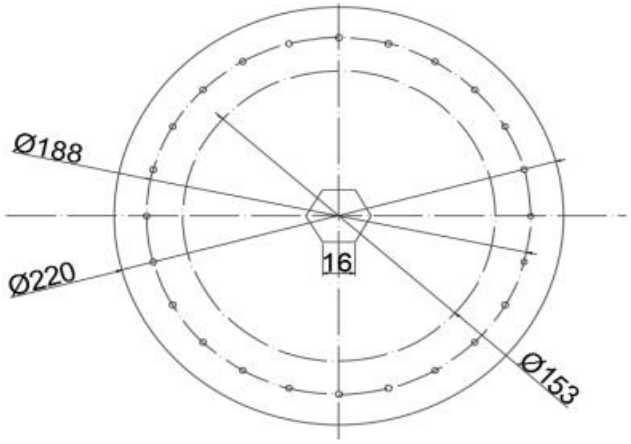

Figure 3. Pneumatic seed discs.

The diameter of the seeding disc ranges from 140 mm to 260 mm [11]. An excessively large or small diameter of the pneumatic seeding disc negatively affects the performance of the pneumatic seeding mechanism. Specifically, when the plant spacing and the marching speed are constant, an excessively small diameter speeds up the rotation of the pneumatic seeding disc. Such condition is unfavorable for the suction of the pneumatic seeding disc, increasing the missing rate. On the contrary, an increased diameter of the seeding disc enables more processing holes, which slows down the pneumatic seeding disc, increases the seed suction rate, and reduces the missing rate [12]. In addition, it will increase the negative pressure cavity and the load of the fan. In this paper, the diameter of the pneumatic seeding disc is designed as 220 mm. The position of the holes should be away from the center of the pneumatic seeding disc maximally, because a closer position will lead to excessive vegetable seeds remaining. In this paper, the diameter of the circle where the holes are located is designed as 188 mm, and the thickness of the pneumatic seeding disc is 1 mm. In the center, there is a regular hexagon with a side length of 16 mm, which cooperates with the regular hexagon on the transmission shaft of the pneumatic seeding mechanism to drive the rotation of the seeding disc.

The holes of the pneumatic seeding disc and the diameter of the seed suction holes are designed based on the average width of the seed according to the Agricultural Machinery Manual [13]:

$$d = (0.64 - 0.66)b \tag{3}$$

where: d—diameter of suction hole, mm; b—average width of seed, mm. The seed rower designed in this paper mainly sows spherical-like seeds with an average width between 3.5 mm and 4.3 mm, so the diameter of this type of hole is 2.2~2.8 mm.

2.1.2. Honeycomb Seeding Mechanism

(1) Honeycomb seeding disc

The structure of the honeycomb seeding disc is shown in Figure 4. It is key to achieving the seeding in two rows. Its main body is a cylinder, with cylindrical holes of the same diameter punched at a certain angle from the two bottom surfaces of the cylinder. An excessively large diameter of seeding disc may result in missed seeding under the centrifugal force. Currently, the available diameter is generally 140–260 mm. The motion trajectory of seeds dropping from the pneumatic seeding mechanism is influenced by external factors, including wind force and mechanical vibration. Thus, holes with a large diameter increase the difficulty for the seed to drop into. Therefore, in this paper, based on the above analysis, the diameter of the holes for the honeycomb seeding disc is designed as 150 mm.

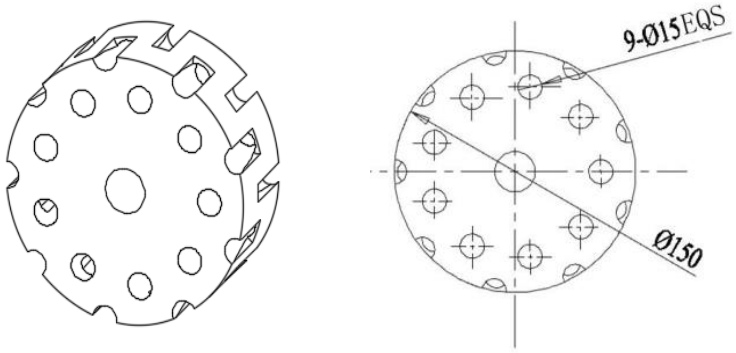

Figure 4. Honeycomb seeding trays.

(2) Seed sorting bin

Based on the diameter of the honeycomb seeding disc, the maximum diameter and width of the seed sorting bin are set to 200 mm and 22.5 mm, respectively. There is a quarter ring in the seed sorting bin, and the difference in the radii of the ring is equal to the diameter of the hole. A quarter of the circle is placed in the first half of the honeycomb seeding disc, as shown in Figure 5. The seed sorting bin is fixed and does not rotate with the rotation of the honeycomb seeding disc, during which the seeds continuously drop into the seeding cavity through the connection of the inclined holes and the quarter ring.

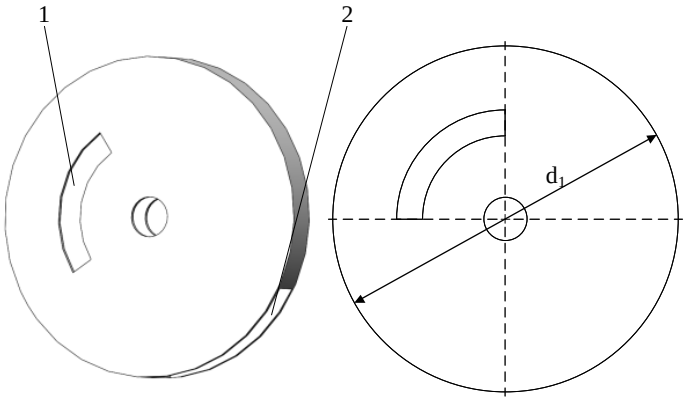

Figure 5. Composition of sub-bin structure. 1. quarter circle; 2. seeding holes.

2.2. Operating Principle

During the operation, a plastic hose is connected to the negative-pressure air inlet of the pneumatic seeding mechanism and the high-pressure vortex fan. The negative-pressure air inlet is connected to the negative-pressure cavity of the right end cover, with sealing rings between them to reduce the missing air. When the seeds are delivered to the seeding area, the negative pressure disappears instantly so that the seeds drop into the inoculation hopper and then pass through the holes under the action of gravity. The holes of the honeycomb seeding disc are connected to the seed sorting bin with a trencher below. In this combined way, the seeding operation is completed. There is a distance between the two rows of seeds, so they are arranged alternately.

2.3. Operating Process

2.3.1. Seeding

Under the effects of negative pressure, the seeds are sucked iton the holes of the pneumatic seeding disc and rotate to the seeding area. They then fall into the inoculation hopper and the holes of the honeycomb seeding mechanism, and then pass through the seed sorting bin. In this paper, a seed is regarded as a particle, and the point where the seed leaves the feeding hole is set as the origin. Meanwhile, the marching direction of the planter

is undertaken as the positive *X*-axis direction, and the vertically downward direction is the positive *Y*-axis direction [14]. The honeycomb and the pneumatic seeding mechanisms are installed on the planter without relative movement, so they are stationary relative to the planter. Thus, influence from the speed of the planter is not considered herein. Furthermore, the air resistance can be ignored because there is a plastic shell coverage when the seeds drop into the honeycomb seeding mechanism. The seed dropping trajectory is shown in Figure 6.

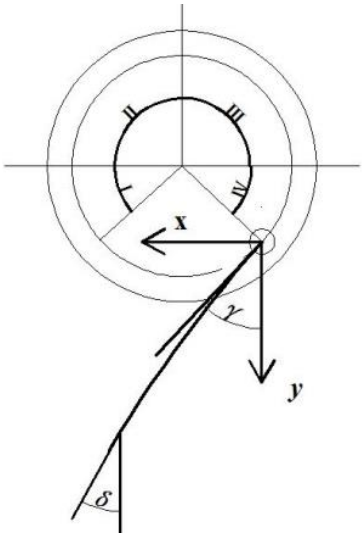

Figure 6. Falling trajectory analysis.

When the seed leaves the seeding area, the velocities in the *X* and *Y* directions are as follows:

$$\begin{cases} V_x = \frac{2\pi n}{60} D_2 sin\gamma \\ V_y = \frac{2\pi n}{60} D_2 cos\gamma \end{cases} \tag{4}$$

The resultant velocity of the seed in contacting with the honeycomb seeding disc is expressed as follows:

$$\begin{cases} V'_x = \frac{2\pi n}{60} D_2 sin\gamma \\ V'_y = \frac{2\pi n}{60} D_2 cos\gamma + \frac{1}{2} gt \end{cases} \tag{5}$$

where: n—rotational speed of the pneumatic seed disc, r/min; D_2—diameter of the index circle where the seed disc hole is located, mm; g—acceleration of gravity, m/s^2; γ—angle of the seed with the vertical direction when it is first thrown, rad; t—time of seed drop, s; Vx—seed velocity in x-direction when leaving the seed drop, m/s; Vy—seed velocity in y-direction when leaving the seed drop, m/s; $V'x$—the partial velocity in the x-direction when the seed touches the honeycomb seed tray, m/s; $V'y$—the partial velocity in the y-direction when the seed touches the honeycomb seed tray, m/s.

Hopping speed when seeds touch the honeycomb seed discharge tray:

$$V = \sqrt{V_x^2 + V_y^2} = \sqrt{\left(\frac{2\pi n}{60} D sin\gamma t\right)^2 + \left(\frac{2\pi n}{60} D cos\gamma + \frac{1}{2} gt\right)^2} \tag{6}$$

The angle between the resultant velocity and the vertical direction when the seeds contacts with the honeycomb seeding disc is given as follows:

$$\delta = \arctan\left(\frac{V'_x}{V'_y}\right) \tag{7}$$

The below expression shows the motion trajectory of the seed when it leaves the pneumatic seeding mechanism and contacts with the honeycomb seeding disc:

$$\begin{cases} S_x = \frac{2\pi n}{60} D sin\gamma t \\ S_y = \frac{2\pi n}{60} D cos\gamma t + \frac{1}{2} g t^2 \end{cases} \quad (8)$$

where: V—the combined velocity of the seeds when contacting the honeycomb seeding disc, m/s; δ—the angle between the combined velocity and the vertical direction when the seeds are in contact with the honeycomb seeding disc, °; S_x—the displacement from the seeds leaving the pneumatic seeding mechanism to contacting the honeycomb seeding disc in the x direction, m; S_y—displacement from the seed leaving the pneumatic seed releasing mechanism to the contacting honeycomb seed releasing disc in the y direction, m.

When contacting with the honeycomb seeding disc, the seeds will collide and bounce, which greatly lowers the success rate of precision seeding. The speed of the seed when contacting the honeycomb seeding disc is affected by the rotational speed of the pneumatic seeding disc and the distance between the honeycomb and the pneumatic seeding mechanisms. The faster the rotation of the pneumatic seeding disc, the greater the initial velocity of the seed when it leaves the pneumatic seeding mechanism. The larger the installation distance between the pneumatic and honeycomb seeding mechanisms, the faster the seed falls under gravity. These two factors increase the chances of seeds contacting the honeycomb seeding apparatus. Therefore, it is recommended to minimize the rotating speed of the pneumatic seeding mechanism and the distance between it and the honeycomb seeding mechanism if possible.

The time of seed dropping can be calculated based on the partial velocities in the x-axis and y-axis directions and the distance between the pneumatic and honeycomb seeding mechanisms. Thus, the falling trajectory of the seeds can be calculated with the trajectory equation, based on which the relative installation position between the pneumatic and honeycomb seeding mechanisms can be determined.

2.3.2. Seed Dropping

After dropping from the feeding hole of the pneumatic seeding mechanism, the seed will pass through the inoculation hopper of the honeycomb seeding mechanism and drop into the holes of the honeycomb seeding disc. To help the seed drop smoothly, the seed dropping is analyzed theoretically, and the optimal inclination angle of the holes is calculated. The force analysis is demonstrated in Figure 7. The static and dynamic friction coefficients between particles and the wall are 0.43 and 0.03, respectively, and the recovery coefficient between them is 0.56 [15].

$$\begin{cases} f_2 = \mu N_2 \\ G \geq \mu N_2 \\ J_2 = m\omega^2 \\ N_2 = (G - J_2)\cos\theta \end{cases} \quad (9)$$

where: u—friction factor between seed and honeycomb seeding disc; θ—slanting angle of honeycomb seeding disc hole, °; N_2—supporting force of seed by slanting cylindrical hole, N; G—gravity of seed itself, N; J_2—seed centrifugal force in honeycomb seeding disc, N; f_2—frictional force of seed in the hole, N; Note: J_2 is always the reverse of the radial direction of the honeycomb seed tray. By calculating the angle of inclination of the type hole to 2°, the seeds can fall from the type hole of the honeycomb seed tray.

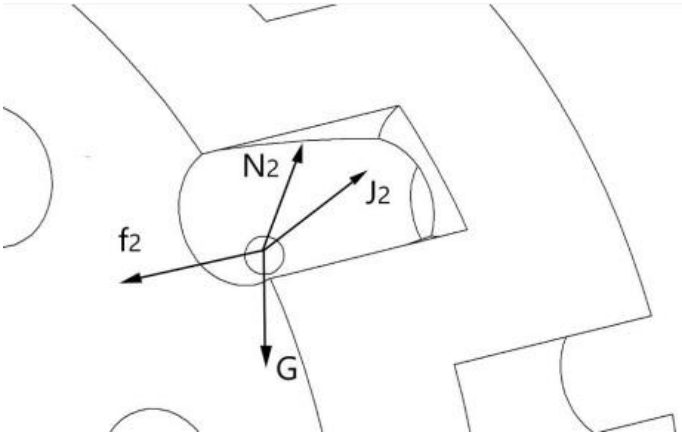

Figure 7. Stress analysis of seed in the hole of mechanical seeding disc.

3. Materials and Methods

3.1. Automatic Dynamic Analysis of Mechanical Systems (ADAMS) Virtual Experiment

For the pneumatic seeding mechanism, the experiment simulates the seeds being adsorbed on the seeding disc, so the stirring wheel, black washer, seed blocking plate, and seed scraping plate can be removed. That is, only the front cover, rear cover, seeding disc, and seeding plate are kept [16,17]. The main part of the honeycomb seeding mechanism is retained and a driving pair is equipped. The simplified pneumatic and honeycomb seeding mechanisms are introduced into ADAMS [18,19]. After the three-dimensional (3D) model of the combined seeding apparatus is imported into ADAMS, the material properties of the honeycomb seeding apparatus are set. After that, the system will automatically calculate the centroid position and rotational inertia of each component for solving dynamics. Each component is renamed for easier identification [20]. After the addition of constraints to each component, drivers were supplemented for the pneumatic and honeycomb seeding discs. In this case, the rotating speeds of these two discs are subject to a proportional relationship.

3.2. Bench Experiments

To obtain the optimal parameter combination of the combined seeding apparatus, performance tests were conducted on the speed of the pneumatic seeding disc, the diameter of the holes, and the vacuum degree of the air cavity of the pneumatic seeding mechanism in the early stage. In addition, single factor and orthogonal experiments were performed on the number and diameter of holes and the seeding height of the honeycomb seeding disc.

In this paper, okra seeds were selected as experimental materials. To achieve better experimental results, the okra seeds were screened based on a purity of $\geq$95% and moisture of $\leq$8%.

The testing instruments include the combined seeding apparatus, a negative-pressure fan, a speed tester, a high-precision digital pressure gauge, a U-shaped pressure gauge, glass glue, a hose, a servo motor (130ST-M10015), a high-speed camera (FASTCAM MiNi WX50 type675KM-16, HOTON, Tokyo, Japan), lighting devices, and a control cabinet. In this paper, for the high-speed camera, the maximum recording speed is 67,500 frames per second (FPS), the recording capacity is 16 G, and the recording speed is 125 FPS. The testing instruments are shown in Figure 8.

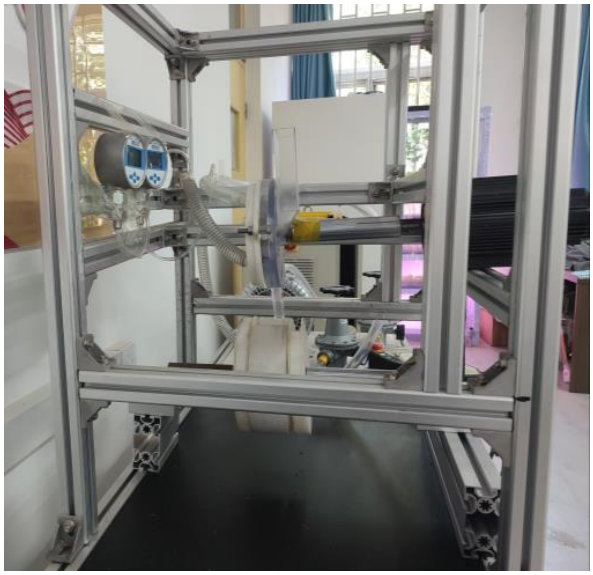

Figure 8. Test bench.

3.3. Test Indicators and Methods

Based on the GB/T6973-2005 "Test Methods for Single Grain (Precision) Planters", the successful seeding rate, missed seeding rate, and re-seeding rate were determined to verify the performance of the precision seeding apparatus [21,22].

The formula for calculating the indicator is as follows:

$$U = \frac{m_1}{M'} \times 100\% \tag{10}$$

where: U—seed casting pass rate, %; m_1—number of qualified seeds in the experiment; M'—total number of samples.

$$V = \frac{m_2}{M'} \times 100\% \tag{11}$$

where: V—missed cast rate, %; m_2—number of missed seeds in the test.

$$W = \frac{m_0}{M'} \times 100\% \tag{12}$$

where: W—re-casting rate; m_3—number of reabsorbed seeds in the experiment.

3.4. Experimental Design

3.4.1. Single Factor Experiments

The test reveals that the pneumatic seeding mechanism performs best when the speed is 18 r/min, the vacuum degree of the air chamber is 3.5 kPa, and the diameter of the holes is 2.4 mm. When the pneumatic seeding mechanism operates at the optimal level, it is combined with the honeycomb seeding mechanism. To determine the optimal operating state of the combined seeding apparatus for precision seeding in two rows, a single factor experiment was conducted with a honeycomb seeding apparatus. During the experiment, the numbers of holes were 12, 18, and 24; the diameters of the holes were 11 mm and 13 mm; and the seeding heights were 60 mm, 80 mm, and 100 mm. After the test bench ran stably, 300 seeds were experimented on, and the experiment was repeated 10 times at each level, based on which the average value was calculated.

3.4.2. Orthogonal Experiments

The results of the single factor experiment revealed that the number of holes, the diameter of the holes, and the seeding height of the honeycomb seeding apparatus exert crucial effects on the operating performance of the combined seeding apparatus. Thus,

they were subjected to orthogonal experiments to determine their influencing order that affects the operating parameters of the experimental indicators and to obtain the optimal operating parameter combination for the combined seeding apparatus. It aims to give a theoretical basis for the optimal running of the combined seeding apparatus [23]. The levels of orthogonal experimental factors are shown in Table 1. Three hundred seeds were experimented on, and the experiment was repeated 10 times at each level, based on which the average value was calculated.

Table 1. Orthogonal test factor level.

Level	Factors		
	Number of Type Holes (A)/pc	Type Hole Diameter (B)/mm	Seeding Height (C)/mm
1	12	11	60
2	18	13	80
3	24	15	100

3.4.3. Double-Row Experiments

After obtaining the optimal parameter combination of the combined seeding apparatus, a double-row experiment was performed on a single disc. Herein, the vertical distance between the honeycomb seeding mechanism and the conveyor belt was set as 130 mm for the experiment. In addition, the speed of the conveyor belt was 10 r/min, 20 r/min, and 30 r/min, and the plant spacing and row spacing were selected as the experimental indicators. The experiment was repeated 10 times, and the average value was calculated and recorded.

3.4.4. High-Speed Photography Experiments

The purpose of the high-speed photography experiment is to observe the condition of the seeds throughout the seeding. Due to the fast rotation of the apparatus, the suction and seeding of seeds by the holes are difficult to observe. In this paper, a high-speed camera was adopted to photograph the seeding process and observe the motion of the seeds in the connection section between the pneumatic and honeycomb seeding mechanisms [24–28].

4. Experiments Results and Discussion

4.1. Results of ADAMS Virtual Simulation

4.1.1. Virtual Experiment of Seed Dropping Trajectory

The seed dropping trajectory is demonstrated in Figure 9. In the pneumatic seeding mechanism, the seeds drop in sequence with the rotation of the seeding disc, and they accurately drop into the holes in the honeycomb seeding disc that continuously rotates. The holes in the honeycomb seeding disc correspond to those in the pneumatic seeding disc, and no missed feeding occurred.

4.1.2. Virtual Experiments with Different Numbers of Holes

As long as a pneumatic seeding mechanism is designed, the number of holes on the pneumatic seeding disc is fixed. Therefore, an excessively small number of holes on the honeycomb seeding disc will cause missed feeding at a constant speed of the pneumatic seeding mechanism. An excessively large number of holes may cause seeds to drop into adjacent holes, resulting in re-seeding. Therefore, the number of holes in the honeycomb seeding disc importantly affects the seeding success rate. Based on the preliminary experimental results, the speed of the pneumatic seeding mechanism was set to 18 r/min, and the number of holes in the honeycomb seeding disc was 12, 18, and 24. The simulation results show that all 24 seeds dropped into the holes, but 7, 5, and 4 seeds bounced out when the number of holes was 12, 18, and 24, respectively. Thus, the corresponding seeding success rates are 70.1%, 79.2%, and 83.3%. The results indicate that as the number of seeds increases, the seeding success rate increases, with the highest

value achieved when there are 24 holes. Therefore, the optimal number of holes in the honeycomb seeding disc is determined as 24.

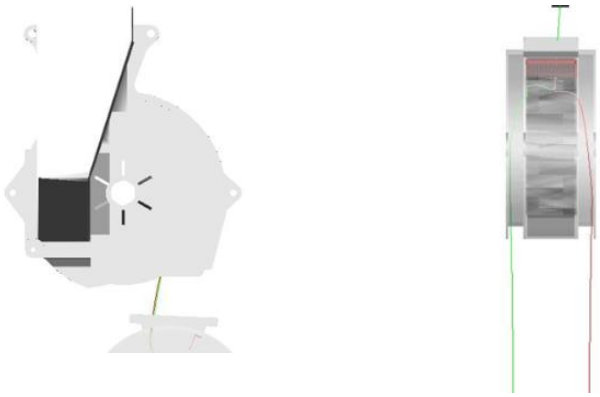

Figure 9. Seed fall trajectory.

4.1.3. Virtual Experiments with Different Diameters of Holes

As mentioned above, the diameter of holes in the honeycomb seeding disc significantly affects the seeding success rate. On the one hand, an excessively small diameter of holes will increase the difficulty for seeds to drop into the holes, reducing the seeding success rate. On the other hand, as the diameter of the hole increases, spacing among the holes decreases, which can easily cause multiple seeds to drop into the same hole. Therefore, virtual experiments were performed on different hole diameters (11 mm, 13 mm, and 15 mm) to determine the optimal diameter. The simulation results showed that all 24 seeds dropped into the holes, but 5, 4, and 4 seeds bounced out at hole diameters of 11, 13, and 15 mm, respectively. Thus, the corresponding seeding success rates were 79.1%, 83.3%, and 83.3%, respectively. The seeding success rate increases with the increased diameter of holes but is the same at the diameter of 13 and 15 mm. Therefore, the diameter of the hole was determined in subsequent bench tests.

4.1.4. Virtual Experiments at Different Seeding Heights

The installation distance between the pneumatic and honeycomb seeding mechanisms is another key factor that affects the seeding success rate. An excessively large distance between the pneumatic and honeycomb seeding mechanisms is not conductive to the seeds dropping into the holes in the honeycomb seeding disc, while a too small distance is not beneficial for installing the mechanisms. Therefore, simulation experiments were conducted using a honeycomb seeding disc with 24 holes, a rotating speed of 18 r/min, and installation distances of 60 mm, 80 mm, and 100 mm. The results indicate that the seeding success rate is the same (83.3%) for the three different installation distances. Under ideal conditions, a small height difference exerts a slight impact on the qualification rate of seeding. However, the actual seeding results may be affected by several uncontrollable factors, such as wind. Therefore, the distance between the two seeding mechanisms should be minimized as much as possible to minimize the influence on seeding. In this paper, it is selected as 60 mm.

4.2. Single Factor Experiments

(1) The Effect of the Number of Holes in Honeycomb Seeding Discs on Seeding

The experimental results in Figure 10 reveal that the seeding success rate increases with the increasing number of holes in the honeycomb seeding disc, while the missed seeding and re-seeding rates are reduced continuously. When the number of holes is 24, the seeding success rate is 82.58%, the missed seeding rate is 8.21%, and the re-seeding rate is 9.21%. These results suggest that the combined seeding apparatus is in the optimal performance state.

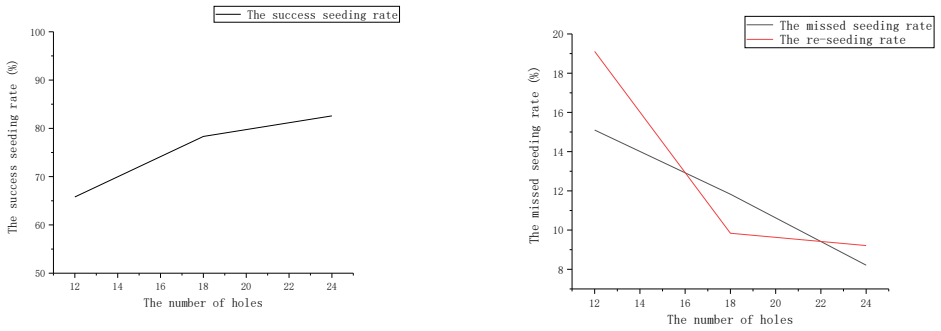

Figure 10. The relationship of the number of honeycomb seeding disc holes.

(2) The Influence of the Diameter of Holes in Honeycomb Seed Discs on Seeding

The experimental results in Figure 11 disclose that the seeding success rate increases with the enlarged diameter of the holes in the honeycomb seeding disc. When the diameter of hole is 15 mm, the seeding success rate is the highest (82.58%), and the re-seeding rate (9.21%) and missed seeding rate (8.21%) are the lowest. The analysis indicates that the increased diameter of holes in the honeycomb seeding disc enlarges the range of seeding, which is beneficial for improving the seeding success rate.

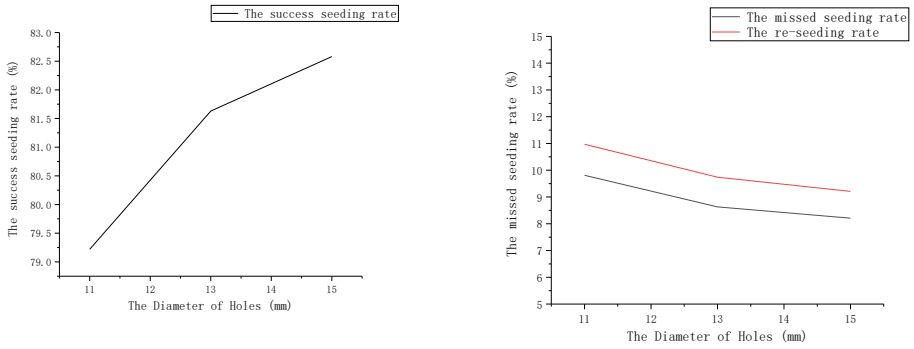

Figure 11. The relationship curve of the diameter of the honeycomb seeding disc hole.

(3) The Impact of Seeding Height on Seeding

As demonstrated in Figure 12, the seeding success rate decreases with the elevating seeding height. When the seeding height is 60 mm, the seeding success rate is 82.58%, which is the highest. When the seeding height is 100 mm, the minimum qualification rate for seeding is 80.56% and the minimum missed seeding rate is 7.36%. Therefore, with the continuously increased seeding height, the seeding qualification rate decreases insignificantly. A comprehensive balance analysis of the above results demonstrates that when the seeding height is 60 mm, the seeding success rate is the highest (82.58%), the missed seeding rate is 8.21%, and the re-seeding rate is 9.21%.

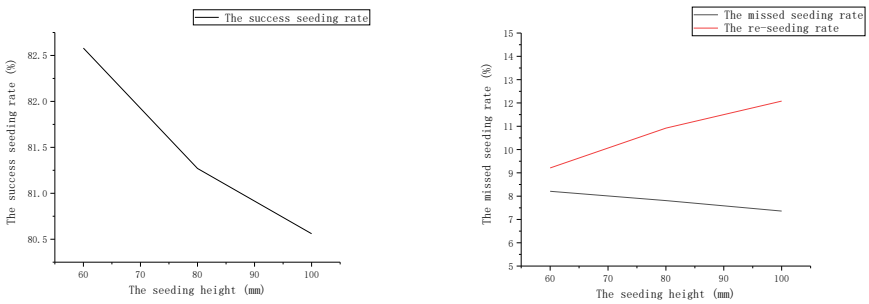

Figure 12. Relationship curve planting height.

4.3. Orthogonal Experiments

(1) The orthogonal experimental scheme and results are listed in Table 2.

Table 2. Orthogonal test scheme and test results.

A	B	C	The Seeding Success Rate/%	The Missed Cast Rate/%	The Re-Injection Rate/%
1	1	1	78.78	10.67	13.55
1	2	2	78.62	11.89	12.49
1	3	3	78.53	12.86	10.61
2	1	2	80.33	6.32	6.35
2	2	3	86.98	5.51	5.51
2	3	1	88.33	6.83	2.84
3	1	3	89.67	4.16	4.17
3	2	1	92.63	3.63	2.74
3	3	2	92.27	2.81	3.92

(2) Results and Analysis

Table 3 shows the range analysis data of the seeding success rate. As shown, A3, B3, and C1 are the optimal levels of factors A, B, and C at $k_{D3} > k_{D2} > k_{D1}$, $k_{E3} > k_{E2} > k_{E1}$, and kF1 > kF3 > kF2, respectively. The higher the qualification rate of seeding, the better the operating performance of the combined seeding apparatus. Therefore, the optimal level for seeding success rate is A3B3C1 and 16.88 > 1.78 > 1.17. The results indicated that the number of holes exerts the greatest effect on the successful seeding, followed by the diameter of holes and the seeding height in turn. Analysis of the range of missed seeding rates reveal that A3, B2, and C2 are the optimal levels of factors A, B, and C at $k_{D1} > k_{D2} > k_{D3}$, $k_{E3} > k_{E1} > k_{E2}$, and $k_{F3} > k_{F1} > k_{F2}$, respectively. The lower the missing rate, the better the operating performance of the combined seeding apparatus. Therefore, the optimal combination for the missed seeding rate is A3B2C2, with 8.27 > 0.50 > 0.49. This indicates that the number of holes exhibits the greatest impact on the missed seeding rate, followed by the seeding height and the diameter of holes in turn. In addition, analysis on the range of re-seeding rates suggests that A3, B3, and C1 are the optimal levels of factors A, B, and C at $k_{D1} > k_{D2} > k_{D3}$, $k_{E1} > k_{E2} > k_{E3}$, and $k_{F2} > k_{F3} > k_{F1}$, respectively.

Table 3. Range analysis of orthogonal test results.

	η1			η2			η3		
	A	**B**	**C**	**A**	**B**	**C**	**A**	**B**	**C**
K1	191.93	218.78	223.74	50.42	36.15	36.13	57.65	45.07	40.13
K2	230.64	222.23	220.22	33.66	36.03	36.02	35.70	41.74	43.76
K3	242.57	224.13	221.18	25.60	37.50	37.53	31.83	38.37	41.29
k1	63.98	72.93	74.58	16.81	12.05	12.04	19.22	15.02	13.38
k2	76.88	74.08	73.41	11.22	12.01	12.01	11.90	13.91	14.59
k3	80.86	74.71	73.73	8.53	12.50	12.51	10.61	12.79	13.76
R	16.88	1.78	1.17	8.27	0.49	0.50	8.61	2.23	1.21

Similarly, the lower the seeding rate, the better the operating performance of the combined seeding apparatus. Thus, the optimal combination for a successful seeding rate is A3B3C1, with 8.61 > 2.23 > 1.21. This means that the number of holes has the greatest impact on the re-seeding rate, followed by the diameter of holes and the seeding height in turn.

Table 4 displays the variance of results of the orthogonal experiments. According to the table, $F_{0.1}$ (2, 6) = 3.46 is obtained. Comparison between it and the F-value in Table 4 demonstrates that all the above three factors can affect the seeding success rate, of which the number of holes in the honeycomb seeding disc exhibits the most significant impact, while the diameter of holes and seeding height show slight impacts. Furthermore, it is

observed that all these three indicators affect the missed seeding rate and the re-seeding rate, with the number of holes exerting the greatest effects.

Table 4. Analysis of variance of orthogonal experiment results.

Mutation Source	SS			df			MS			F-Value		
	η_1	η_2	η_3	η_1	η_2	η_3	η_1	η_2	η_3	η_1	η_2	η_3
A	467.2	106.88	129.27	2	2	2	233.62	53.43	64.63	195.66	75.98	31.48
B	4.90	0.44	7.48	2	2	2	2.45	0.22	3.74	0.03	0.012	0.17
C	2.20	0.47	2.29	2	2	2	1.10	0.24	1.14	0.01	0.013	0.05

The experimental indicators are required to achieve a higher seeding success rate while minimizing the missed seeding and re-seeding rates maximally. Based on a joint analysis of Tables 3 and 4, the optimal combination is determined as A3B2C1, with a seeding success rate of 81.63%, a missed seeding rate of 8.63%, and a re-seeding rate of 9.74%.

4.4. High-Speed Photography Experiments

Figure 13 illustrates the results of the high-speed photography experiments for the combined seeding apparatus. The figure demonstrates that re-seeding and missed seeding are both observed during the seeding. The missed seeding is attributed to two aspects. On the one hand, the matching between the rotating speed parameters of the pneumatic and honeycomb seeding mechanisms results in a deviation of the seeds accurately dropping into the honeycomb seeding mechanism. On the other hand, the seeds do not drop into the hole in the honeycomb seeding mechanism exactly or even drop out of the mechanism. Meanwhile, two major reasons are summarized for re-seeding. One is that the seeds are stacked in the seed storage box of the pneumatic seeding mechanism and are subjected to compression and friction. In this case, multiple seeds may be sucked by the pneumatic seeding mechanism and then dropped into the honeycomb seeding mechanism. The other is that the seeds may fall on the edge of holes in the honeycomb seeding mechanism and then drop into the adjacent holes.

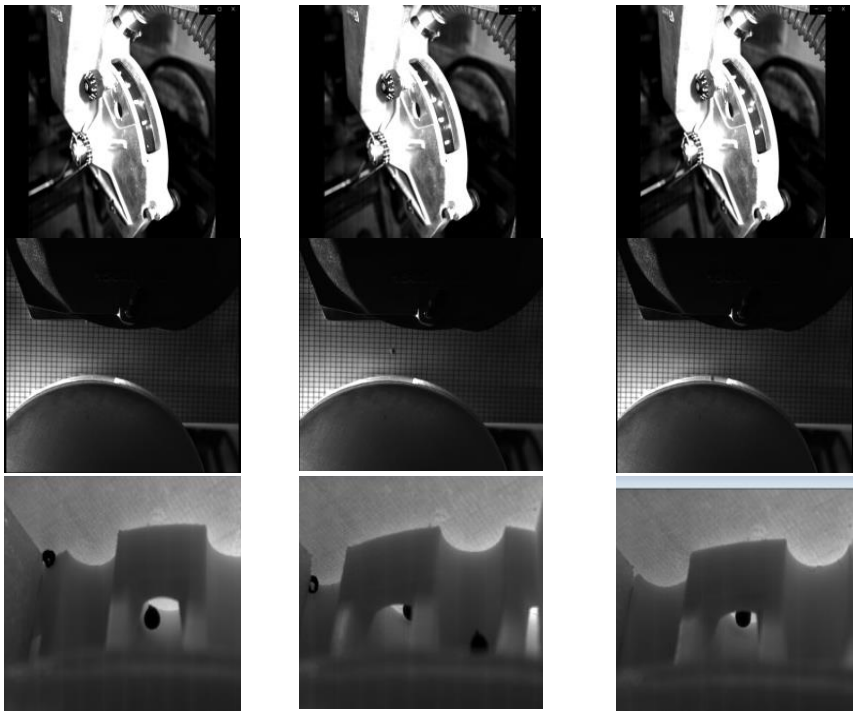

Figure 13. Pictures of high-speed photography test of combined seed metering device.

5. Discussion

The results of the ADAMS virtual experiment suggest that the seeding success rate also increases with an increasing number and diameter of holes in the honeycomb seeding disc. Specifically, the seeding success rate is the highest, reaching 83.3%, when the number of holes in the honeycomb seeding disc is 24 or the diameter of the hole is 13 mm and 15 mm. In addition, it is observed that when the seeding height changes, the seeding success rate of the combined seeding apparatus is 83.3%, indicating that it is basically not affected by the seeding height. Based on joint consideration of external factors, in this paper, the seeding height is set to 60 mm.

The results of the single factor experiment reveal that as the number of holes increases, the seeding success rate of the combined seeding apparatus continuously increases, while the missed seeding and re-seeding rates decrease. When the number of holes is 24, the seeding success rate is 82.58%, the missed feeding rate is 8.21%, and the re-feeding rate is 9.21%. In this case, the combined seeding apparatus reaches the best performance state. As the diameter of the holes increases, the seeding success rate of the combined seeding apparatus continuously increases. When the diameter is 15 mm, the seeding success rate is 82.58%, the missed seeding rate is 8.21%, and the re-seeding rate is 9.21%. The performance of the combined seeding apparatus has reached its optimal state with the highest seeding success rate and the lowest missed seeding and re-seeding rates. As the seeding height increases, the seeding success rate continues to decrease. When the seeding height is 60 mm, the seeding success rate is the highest, reaching 82.58%, the missed seeding rate is 8.21%, and the re-seeding rate is 9.21%. The experimental results are consistent with those of the virtual experiment. Therefore, the research results of the paper are a useful reference for optimizing the operating parameters of the combined seeding apparatus, meeting the operational requirements of vegetable seeding.

Furthermore, the results of the high-speed photography experiment disclose that, during the seeding, the combined seeding apparatus experiences re-feeding and missed feeding. When the speed parameters of the pneumatic and honeycomb seeding mechanisms are not accurately matched, the seeds will not accurately drop into the holes in the honeycomb seeding mechanism and may even fall out of the mechanism, resulting in missed seeding. When the seeds pass through the pneumatic seeding mechanism, excessive air pressure from the fan can cause re-suction of the seeds, resulting in multiple seeds being sucked and dropping into the holes in the honeycomb seeding mechanism. In addition, the seeds with missed seeding will drop on the edge of holes in the honeycomb seeding mechanism and may drop into adjacent holes. These situations can all cause re-seeding in the combined seeding apparatus. The experimental results herein can provide a reference for analyzing the reasons for missed seeding and re-seeding of the combined seeding apparatus.

6. Conclusions

Concerning the low seeding efficiency and poor qualification rate of the current precision seeding apparatus for vegetable seeds, this paper designed a combined seeding apparatus and elaborated its operating principle. On this basis, it theoretically analyzed the operating process of combined seeding apparatus. Meanwhile, virtual experiments were performed on the combined seeding apparatus using ADAMS to simulate the changes in seed drop trajectory and seeding success rate under different structures and operating parameters. Finally, the influences of the number and diameter of the holes and seeding height of the honeycomb seeding mechanism on the operating performance of the combined seeding apparatus were analyzed by taking the bench test. The following conclusions are drawn:

(1) Parameter equations were established for the speed and trajectory of seeds during the seeding for analysis to provide the theoretical foundation for installing the honeycomb seeding mechanism. Accordingly, a parameter equation was offered for the seeds during the seed dropping. It was then found that when the inclination angle of

the holes in the honeycomb seeding disc is 2°, the seed can roll off the honeycomb seeding disc. Therefore, the inclination angle of the hole should be 2° in designing the honeycomb seeding mechanism.

(2) With ADAMS, virtual experiments were performed on the designed combined seeding apparatus under different parameter conditions of the honeycomb seeding apparatus. The results show that when the number and diameter of holes in the honeycomb seeding disc are 24 and 13 mm, respectively, the seeding success rate is the highest, both of which are 83.3%. Meanwhile, the results reveal that the seeding success rates are the same when the installation distances between two seeding mechanisms are different, suggesting that the seeding height presents a slight effect on the seeding success rate. The seeds may be affected by some external factors during dropping, so the distance between the two seeding mechanisms should be minimized as much as possible to reduce the influence on the success seeding.

(3) Based on the single factor and orthogonal experiments on the parameters, the optimal parameter combinations of the combined seeding apparatus were determined. That is, the number and diameter of holes in the honeycomb seeding disc are 24 and 13 mm, respectively, and the seeding height is 60 mm. With these parameter settings, the seeding success rate is 81.63%, while the missed seeding rate and the re-seeding rate are 8.63% and 9.74%, respectively. The double-row seeding shows the best effect when the speed of the conveyor belt is 20 r/min, the row spacing is 80 mm, and the plant spacing is 51 mm. In addition, the high-speed camera shows that re-feeding and missed feeding occur during the running of the combined seeding apparatus.

Author Contributions: Conceptualization, Y.L. and F.X.; methodology, Y.L., software, Y.B.; validation, X.Z.; formal analysis, X.Z.; resources, Y.B. and F.X.; data curation, Y.L., writing—original draft preparation, Y.L.; writing—review and editing, F.X. and Y.L.; funding acquisition, Y.L. and F.X. All authors have read and agreed to the published version of the manuscript.

Funding: This work was mainly supported by the Natural Science Foundation of Shandong Province, ZR2020ME136; Shandong Province Key R&D Program (Major Science and Technology Innovation Project)-Research and Development of High-Efficiency Production Equipment for Specialty Vegetables-2022CXGC010612.

Institutional Review Board Statement: Not applicable.

Data Availability Statement: All data are contained within the article. The data presented in this study can be requested from the authors.

Conflicts of Interest: The authors declare no conflict of interest.

References

1. Zhao, L.J.; Yan, S.S.; Wang, Y.J.; Zhang, Y.X.; Han, Y.M.; Cai, X.H.; Xu, C.L. Design and test of air-suction single and double row precision universal seed metering device. *J. Agric. Mech. Res.* **2019**, *41*, 136–141.
2. Parish, R.L.; Mc Coy, J.E.; Bracy, R.P. Belt-type seeder for soybeans. *Appl. Eng. Agric.* **1999**, *15*, 103–106. [CrossRef]
3. Ess, D.R.; Hawkins, S.E.; Young, J.C.; Christmas, E.P. Evaluation of the performance of a belt metering system for soybeans planted with a grain drill. *Appl. Eng. Agric.* **2005**, *21*, 965–969. [CrossRef]
4. Hu, J.; Mao, H. Principle analysis and experiment of magnetic precision seed metering. *Trans. Chin. Soc. Agric. Mach.* **2004**, *4*, 55–58.
5. Karayel, D.; Ozmerzi, A. Evaluation of three depth-control components on seed placement accuracy and emergence for a precision planter. *Appl. Eng. Agric.* **2008**, *24*, 271–276. [CrossRef]
6. Maleki, M.R.; Mouazen, A.M.; De Ketelaere, B.; De Baerdemaeker, J. A New Index for Seed Distribution Uniformity Evaluation of Grain Drills. *Biosyst. Eng.* **2006**, *94*, 471–475. [CrossRef]
7. Yazgi, A.; Degirmencioglu, A. Optimisation of the seed spacing uniformity performance of a vacuum-type precision seeder using response surface methodology. *Biosyst. Eng.* **2007**, *97*, 347–356. [CrossRef]
8. Zhang, D.G.; Gu, Y.M.; Zheng, D.C.; Cui, Q.L. Development of 2BX-10 type small seed precision seeder. *J. Shanxi Agric. Univ. (Nat. Sci. Ed.)* **2010**, *30*, 459–463.
9. Tian, B.P.; Liao, Q.X.; Huang, H.D.; Shu, C.X.; Duan, H.B.; Li, J.B. Design of 2BFQ-6 type rape precision combined direct seeding machine. *Trans. Chin. Soc. Agric. Mach.* **2008**, *10*, 211–213.

10. Wang, Z.Q.; Wu, L.H.; Cao, J.; Yu, B.; Sun, Q.; Xin, G.; Cheng, R. Brief introduction of 2BQX-5 millet suction planter. *Nong Cun Mu Qu Ji Xie Hua* **2015**, *4*, 44–45.
11. Zhang, K.X.; Li, J.F.; Liu, X.X. Optimal design and experiment of variable particle size double disc air-suction precision seed meter. *Trans. Chin. Soc. Agric. Mach.* **2019**, *50*, 52–63.
12. Wei, H.M.; Yang, F.Z.; Li, J.D.; Yang, W.; Luo, J.; Liu, X.C. Design and test of suction vertical disc rice precision seed metering device. *Agric. Eng.* **2018**, *8*, 93–96.
13. Chinese Academy of Agricultural Mechanization Sciences. *Agricultural Machinery Design Manual Volume One*; China Agricultural Technology Press: Beijing, China, 2007.
14. Jia, H.L.; Chen, Y.L.; Zhao, J.L.; Wang, J.X.; Guo, M.Z.; Zhuang, J. Design and Test of Air Suction Mechanical Compound Soybean Precision Metering Device. *Trans. Chin. Soc. Agric. Eng.* **2018**, *49*, 75–86+139.
15. Liu, H.X.; Liu, J.X.; Tang, S.F.; Xu, X.M. Design of high-speed precision soybean seed metering device with opposed swash plate and analysis of seed filling mechanism. *Trans. Chin. Soc. Agric. Eng.* **2016**, *32*, 24–31.
16. Zhang, X.L.; Song, J.; Li XY Xie, F.X.; Zhang, L. Design and simulation analysis of pneumatic mechanical combined single disc and double row seed meter. *J. Chin. Agric. Mech.* **2020**, *41*, 30–34. [CrossRef]
17. Wang, F.Y. Simulation research on conveyor cleaning device for sugar beet based on ADAMS. *J. Chin. Agric. Mech.* **2016**, *37*, 57–61.
18. Zhang, J.; Wang, Y.; Huang, M.; Wang, S.H. Experiment and simulation of coleseed filling angle based on ADAMS. *J. Chin. Agric. Mech.* **2015**, *36*, 46–49.
19. Tang, H.; Xu, F.D.; Xu, C.S.; Zhao, J.L.; Wang, Y.J. The influence of a seed drop tube of the inside-filling air-blowing precision seed-metering device on seeding quality. *Comput. Electron. Agric.* **2023**, *204*, 107555. [CrossRef]
20. Yuan, H.; Fang, W.; Zhang, Q.L.; Liang, B.K.; Yao, L. Kinematic analysis and simulation of 4-axis stamping handling robot based on ADAMS. *J. Chin. Agric. Mech.* **2018**, *46*, 24–27,123.
21. Gan, Y.; Stobbe, E.H. Effect of variations in seed size and planting depth on emergence, infertile plants, and grain yield of spring wheat. *Rev. Can. De Phytotech.* **1995**, *75*, 565–570. [CrossRef]
22. Camacho-Tamayo, J.H.; Barbosa, A.M.; Pérez, N.M.; Leiva, F.R.; Rodríguez, G.A. Operational characteristics of four metering systems for agricultural fertilizers and amendments. *Eng. Agric.* **2009**, *29*, 605–613. [CrossRef]
23. Tang, H.; Xu, C.S.; Xu, W.L.; Xu, Y.N.; Xiang, Y.S.; Wang, J.W. Method of straw ditch buried returning, development of supporting machine and analysis of influencing factor. *Front. Plant Sci.* **2022**, *13*, 967838. [CrossRef] [PubMed]
24. Yuan, Y.M.; Ma, X.; Zhu, Y.H.; Wang, C.H.; Dong, R.J.; Wang, J.L. Analysis of seeding process of air suction seed metering device based on high-speed camera technology. *J. Jilin Agric. Univ.* **2008**, *4*, 617–620.
25. Yu, J.J.; Ding, Y.C.; Liao, Y.T.; Cong, J.L.; Liao, Q.X. Analysis of seeding trajectory of pneumatic rape precision metering device based on high-speed camera. *J. Huazhong Agric. Univ.* **2014**, *33*, 103–108.
26. Wang, Z.M.; Luo, X.W.; Huang, S.X.; Chen, W.T.; Li, J.H. High-speed camera analysis of the filling process of the hole type rice seeding wheel. *Trans. Chin. Soc. Agric. Eng.* **2009**, *40*, 56–61.
27. Tang, H.; Xu, C.S.; Wang, Z.M.; Wang, Q.; Wang, J.W. Optimized design, monitoring system development and experiment for a long-belt finger-clip precision corn seed metering device. *Front. Plant Sci.* **2022**, *13*, 814747. [CrossRef]
28. Bao, Y.F.; Wang, F.Y.; Jiang, J.T.; Chen, F. Research progress and development trend of precision seeding equipment for vegetable seeds. *J. Agric. Mech. Res.* **2021**, *43*, 247–254.